Dynamic Mechanical Properties and Morphology of High-Density Polyethylene/$CaCO_3$ Blends With and Without an Impact Modifier

Yu-Lin Yang,[1] Christian G'Sell,[2] Jean-Marie Hiver,[2] Shu-Lin Bai[1]

[1]*Center for Advanced Composite Materials, Department of Advanced Materials and Nanotechnology, State Key Laboratory of Turbulence and Complex Systems, College of Engineering, Peking University, Beijing 100871, People's Republic of China*
[2]*Laboratoire de Physique des Matériaux, Ecole des Mines de Nancy, Parc de Saurupt, 54042 Nancy Cedex, France*

Received 9 August 2006; accepted 9 October 2006
DOI 10.1002/app.25619
Published online in Wiley InterScience (www.interscience.wiley.com).

ABSTRACT: Dynamic mechanical analysis and differential scanning calorimetry were used to investigate the relaxations and crystallization of high-density polyethylene (HDPE) reinforced with calcium carbonate ($CaCO_3$) particles and an elastomer. Five series of blends were designed and manufactured, including one series of binary blends composed of HDPE and amino acid treated $CaCO_3$ and four series of ternary blends composed of HDPE, treated or untreated $CaCO_3$, and a polyolefin elastomer [poly(ethylene-*co*-octene) (POE)] grafted with maleic anhydride. The analysis of the tan δ diagrams indicated that the ternary blends exhibited phase separation. The modulus increased significantly with the $CaCO_3$ content, and the glass-transition temperature of POE was the leading parameter that controlled the mechanical properties of the ternary blends. The dynamic mechanical properties and crystallization of the blends were controlled by the synergistic effect of $CaCO_3$ and maleic anhydride grafted POE, which was favored by the core–shell structure of the inclusions. The treatment of the $CaCO_3$ filler had little influence on the mechanical properties and morphology. © 2006 Wiley Periodicals, Inc. J Appl Polym Sci 103: 3907–3914, 2007

Key words: blends; fillers; mechanical properties; morphology

INTRODUCTION

Adding inorganic particles to polymers is an efficient and cheap method of enhancing their mechanical properties and making them suitable for engineering applications such as structural materials.[1] For this reason, particle-filled polymers have been the objects of sustained interest in industrial and academic research. Among the most used inorganic fillers, calcium carbonate ($CaCO_3$) is widely used to reinforce polymers.[2–7] However, to avoid extensive damage on deformation, it is better to disperse homogeneously the particles in the material and to improve their bonding with the polymer matrix. One method for fulfilling the latter condition is to introduce a rubbery phase into the composite. Thus, polymer composites containing a soft elastomer and a rigid filler present a morphology that corresponds either to core–shell inclusions (with a rubber interphase between the inorganic particles and the polymer matrix) or separately dispersed filler particles and rubber nodules. Several authors have shown that, for such composites, better mechanical properties can be obtained both by the adjustment of the composition and by the tuning of the phase morphology by all available means.[8–12] Premphet and Horanont[8] showed that in polypropylene (PP)/elastomer/filler composites, the phase structure was determined mainly by the chemical character of the components and, to a lesser degree, by the mixing sequences of each component.

In this work, we focus our attention on compounds based on high-density polyethylene (HDPE). Although this commodity polymer exhibits modest performances in its neat form, its properties can be substantially improved when it is blended with other polymers or reinforced with mineral fillers. Also, because of their high tear resistance, poly(ethylene-*co*-octene) (POE) copolymers have attracted more research and are widely used for modifying nonpolar polymers.[13–17] In addition, they can be functionalized or grafted with unsaturated molecules containing polar functional groups such as maleic anhydride. In previous studies, little work has been done on HDPE/POEg/$CaCO_3$ compositions [where POEg is poly(ethylene-*co*-octene) grafted with maleic anhydride]. Here we investigated various composite materials: (1) binary blends of HDPE with $CaCO_3$ particles and (2) ternary blends with $CaCO_3$ and POEg.

Dynamic mechanical analysis (DMA) and differential scanning calorimetry (DSC) were systematically used for determining the mechanical and thermal properties

Correspondence to: S. L. Bai (slbai@pku.edu.cn).
Contract grant sponsor: National Natural Science Foundation of China; contract grant number: 10472002.
Contract grant sponsor: Programme de Recherche Avancée program between China and France.

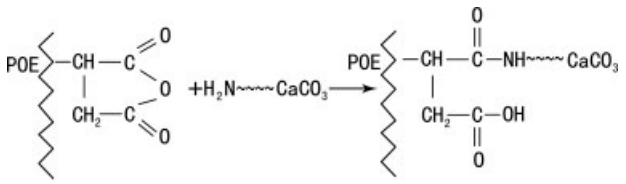

Figure 1 Chemical reaction between POEg and treated $CaCO_3$.

of our materials. The data obtained from both techniques gave access to microstructural features such as the crystallinity, molecular relaxations, miscibility, and morphology. Furthermore, the phase structure of the HDPE composites was investigated with scanning electron microscopy (SEM). Through these approaches, we explore the possible synergistic effects between the filling particles and the rubber phase on the composites.

EXPERIMENTAL

Materials

The HDPE used in this work was a commercial grade (HDPE 5070EA) supplied by Panjin Petrochemical Co. (Panjin City, Liaoning Province, People's Republic of China) (melt flow index = 23 g/10 min). POE (Engage 8445) was supplied by DuPont–Dow Co. (Plaquemine, LA) with 9.5 wt % octene (melt flow index = 3.5 g/10 min). It was subsequently grafted with 1 wt % maleic anhydride at the Institute of Chemistry of the Chinese Academy of Science. The grafted copolymer was called POEg.

Two kinds of fillers were used in this work. The first one was made of plain $CaCO_3$ (untreated) supplied by Heshan Chemical Industrial Co. (Liaoning, People's Republic of China). The mean size of the particles (by number) was about 0.7 μm. The second (treated $CaCO_3$) was the same $CaCO_3$, but its surface was treated with an amino acid to improve adhesion with the polymer matrix. The amino acid (JL GD02) was provided by Nanjing Chemical Industrial University. The acid treatment was performed at 100°C in a high-speed mixing machine for 15–30 min. The layer introduced by this treatment on the surface of the $CaCO_3$ particles represented 2% of the filler weight.

The reaction principle between POEg and treated $CaCO_3$ is based on the interfacial reaction illustrated in Figure 1, in which it cam be seen that the maleic radicals attached to the POE macromolecules react with the NH_2 radicals at the surface of the treated $CaCO_3$ particles. Without this reaction between POEg and the untreated particles, the interfacial strength of the $CaCO_3$/POEg interface is lower.

The materials investigated in this study were obtained by the mixing of two or three of the ingredients (HDPE, POEg, untreated $CaCO_3$, or treated $CaCO_3$) in a high-speed mixing machine for 20 min and then pelletized by means of a twin-screw extruder (diameter = 30 mm) at about 210°C. Their formulations are summarized in Table I. Specimens for DMA and DSC measurement were injection-molded into the shapes of discs 2 mm thick and 100 mm in diameter. The samples for testing were carefully cut from the discs with a milling machine.

DMA

The viscoelastic properties of the materials were investigated with a Netzsch DMA242C dynamical mechanical analyzer (Selb, BaVain, Germany). The DMA tests were run in a dual-cantilever bending mode with samples of the following calibrated dimensions: 9 mm wide, 2 mm thick, and 16 mm long. Temperature–time or stress–strain scans were carried out at a frequency of 1 Hz. The static force was zero, and the maximum dynamic deflection was equal to 100 μm. The starting and ending temperatures were fixed at −150 and +100°C, respectively. A heating rate of 2°C/min was adopted for the temperature/time scans.

DSC

The melting and crystallization behavior of the blends was studied with DSC (DSC 7, PerkinElmer, Wellesley, MA) with specimens whose mass was approximately 8 mg. The heating or cooling sequences were programmed at a rate of 10°C/min. All specimens were first heated to 160°C and held at this temperature for 10 min to erase any thermal memory. Subsequently, they were cooled to 20°C, held at that temperature for

TABLE I
Formulations of the Materials (Weight Fractions)

A series (HDPE/treated $CaCO_3$)		AP series (HDPE/POEg/treated $CaCO_3$)		BP series (HDPE/POEg/untreated $CaCO_3$)		AP30 series (HDPE/POEg/treated $CaCO_3$)		BP30 series (HDPE/POEg/untreated $CaCO_3$)	
No.	Composition	No.	Composition	No.	Composition	No.	Composition	No.	Composition
A0	100/0					AP30-1	66.4/3.6/30	BP30-1	66.4/3.6/30
A10	90/10	AP10	85.5/4.5/10	BP10	85.5/4.5/10	AP30-2	62.8/7.2/30	BP30-2	62.8/7.2/30
A30	70/30	AP30	56.5/13.5/30	BP30	56.5/13.5/30	AP30-3	59.2/10.8/30	BP30-3	59.2/10.8/30
A40	60/40	AP40	42/18/40	BP40	42/18/40	AP30-4	55.6/14.4/30	BP30-4	55.6/14.4/30
A50	50/50	AP50	27.5/22.5/50	BP50	27.5/22.5/50	AP30-5	52/18/30	BP30-5	52/18/30

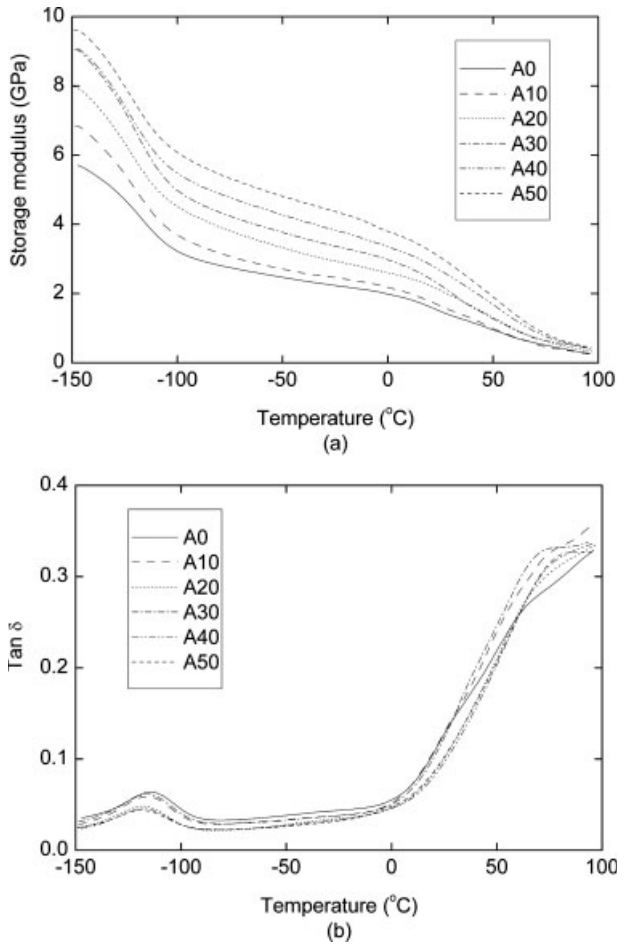

Figure 2 Variation of the viscoelastic properties for neat HDPE and the A series: (a) the storage modulus and (b) tan δ.

2 min, and then subjected to a second heating cycle with conditions identical to those of the first one. Crystallization was analyzed during the cooling part of the thermal cycle and melting during the second heating.

Morphological study

The morphology of the composites was examined with an environmental scanning electron microscope (Quanta 200F, Fei Co., Hillsboro, OR). Nondeformed specimens were first cryofractured. Then, the cryofractured surfaces were etched in normal heptane to remove POE. Subsequently, the surfaces of the composites (etched and nonetched) were examined under the environmental scanning electron microscope to study the morphology. No more treatment was applied to the surfaces before the observation.

RESULTS AND DISCUSSION

Dynamical mechanical analysis

The influence of temperature on the viscoelastic properties of neat HDPE and the A series materials is displayed in Figure 2. The tan δ curve for neat HDPE confirms that the glass-transition temperature (T_g) of the amorphous phase occurs at a very low temperature: T_g is −114.5°C at a frequency of 1 Hz [Fig. 2(b)]. Furthermore, the plateau in the tan δ curve between −90 and 5°C indicates that no further mobility is activated in that temperature range. Above 5°C, tan δ increases gradually because of the progressive activation of crystalline movements (e.g., the migration of Renecker defects) and ultimately the melting of the polymer. As for the effect of $CaCO_3$ addition, Figure 2(a) shows that the storage modulus increases significantly with increasing particle content. At room temperature, for example, the modulus of the blends increases from 1.54 GPa for neat HDPE up to 3.13 GPa for the material with 50 wt % $CaCO_3$. In contrast, Figure 2(b) shows that the addition of $CaCO_3$ has very little influence on tan δ.

The corresponding viscoelastic curves of the AP series, in which the matrix is filled with treated $CaCO_3$ particles and POEg, are displayed in Figure 3. The blends were formulated in such a way that the POEg/treated $CaCO_3$ weight ratio was constantly equal to 0.45. This condition was fixed because the addition of

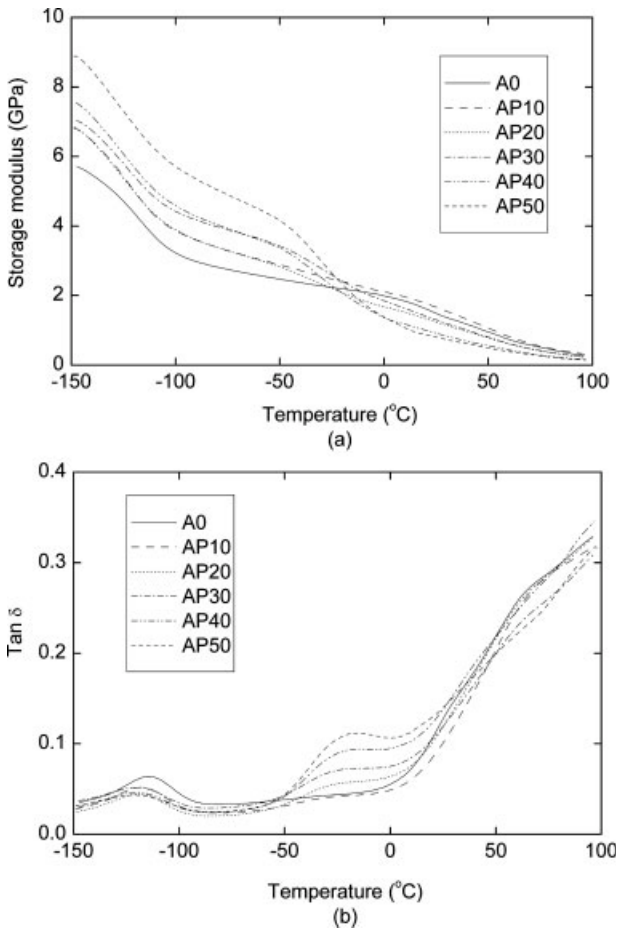

Figure 3 Variation of the viscoelastic properties for neat HDPE and the AP series: (a) the storage modulus and (b) tan δ.

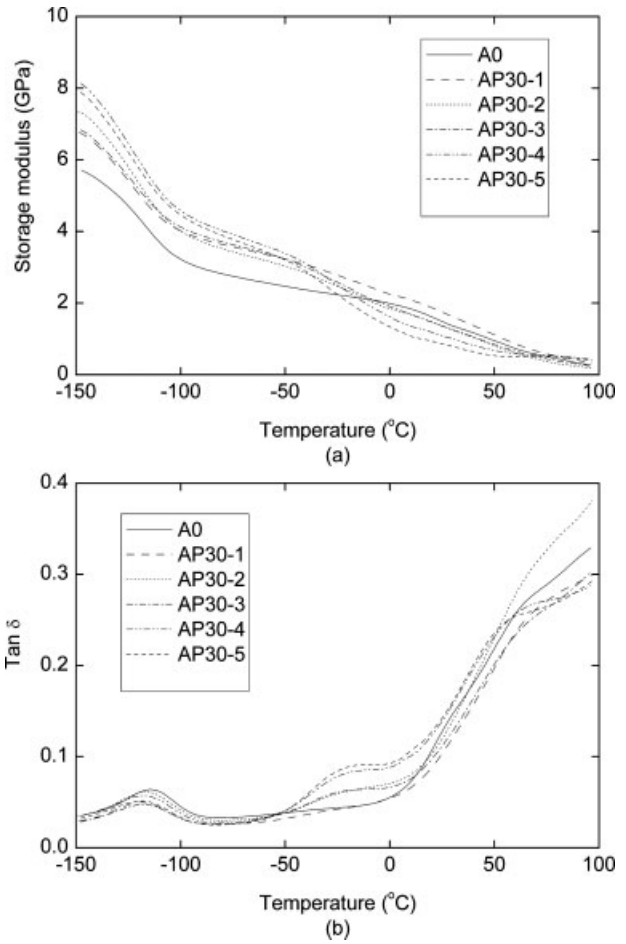

Figure 4 Variation of the viscoelastic properties for neat HDPE and the AP30 series: (a) the storage modulus and (b) tan δ.

POEg to the blends was designed to compatibilize somehow the particle with the polymeric matrix. Figure 3(b) shows that a new peak in tan δ occurs at about −15°C and that the height of this peak increases with the amount of POEg; this indicates that the amount of POEg has a noticeable influence on tan δ. This peak was ascribed to T_g of the polyolefin elastomer. As such, the existence of a well-defined peak is the proof that in the ternary blends distinct phase separation exists. Quite logically, the glass-transition peak of HDPE decreases at the same time as the POEg peak increases. As for the modulus [Fig. 3(a)], the variation with the $CaCO_3$ content is complex. At a low temperature (when POEg is glassy), the modulus increases with the $CaCO_3$ content because of the higher stiffness of the particles. In contrast, in the temperature range in which POEg is rubbery, the modulus decreases as POEg increases, although the $CaCO_3$ content also increases. One exception is AP10, whose modulus is always higher than that of neat HDPE because the POEg content is low and the $CaCO_3$ particles play the preponderant role in this blend. Obviously, the modulus evolution depends on the relative proportion of flexible POEg and rigid $CaCO_3$.

The influence of POEg on the behavior of the materials, for which the $CaCO_3$ amount is constant, is better illustrated by the graphs in Figure 4. In Figure 4(a), below T_g of POEg (i.e., −15°C), the blends exhibit a higher elastic modulus than the neat HDPE. This effect is certainly due to the combined contribution of rigid $CaCO_3$ and glassy POEg. In contrast, above that temperature, the blends are generally more flexible than the neat HDPE, and the modulus decreases with the POEg content. As for the tan δ peak [Fig. 4(b)], its height increases with the amount of POEg. As such, the results shown in Figures 3 and 4 reveal the major role played by POEg, whose glass transition controls the behavior of the blends.

We now check the influence of the particle treatment by comparing the graphs in Figures 3 and 4 for treated $CaCO_3$ with those in Figures 5 and 6 obtained for homologous materials with untreated $CaCO_3$. For example, Figure 7 shows the storage modulus of five series of

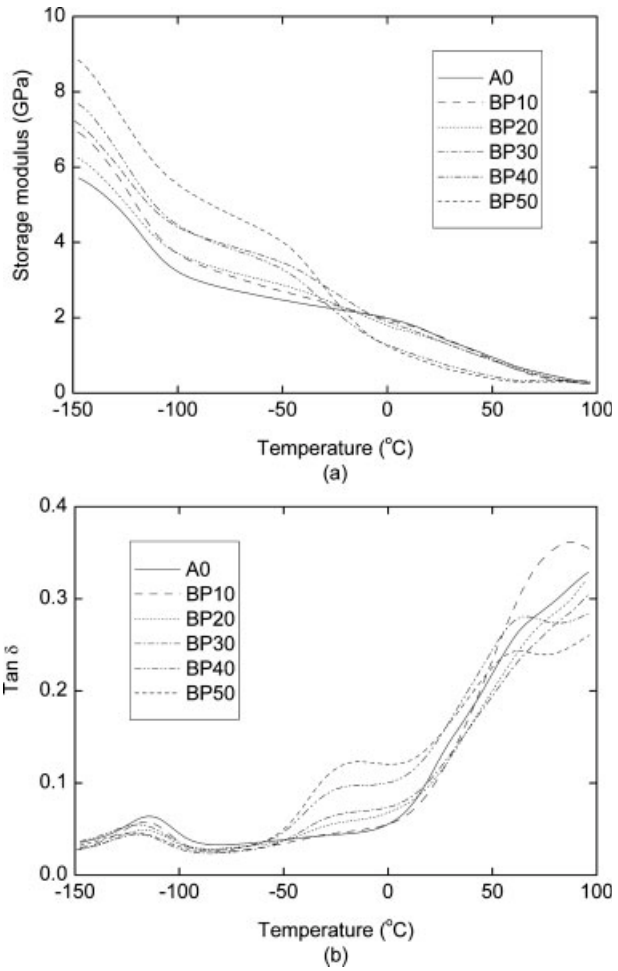

Figure 5 Variation of the viscoelastic properties for neat HDPE and the BP series: (a) the storage modulus and (b) tan δ.

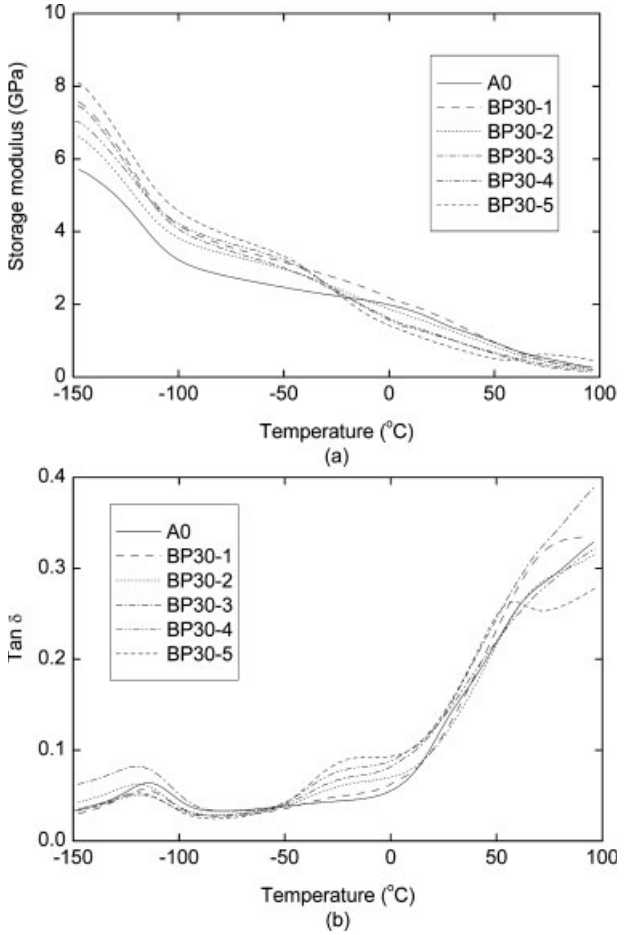

Figure 6 Variation of the viscoelastic properties for neat HDPE and the BP30 series: (a) the storage modulus and (b) tan δ.

blends at room temperature. The tendency shown in the curves agrees with the previous analysis. The particle treatment does not influence significantly the viscoelastic behavior of the blends. This result is in line with the results presented in our previous study devoted to the stress–strain response and volume dilatation of the same materials under uniaxial tension at a constant true strain rate.[18] That investigation showed that neither the Young's modulus nor the cavitation kinetics were significantly influenced by the particle treatment. Only the yield stress was moderately higher for the materials with treated particles because of the higher interfacial adhesion.

DSC

To study the influence of the mineral particles and rubber phase on the melting and crystallization of the HDPE matrix in the blends, DSC studies of the nonisothermal melting and crystallization behavior were performed with the thermal cycle described before.

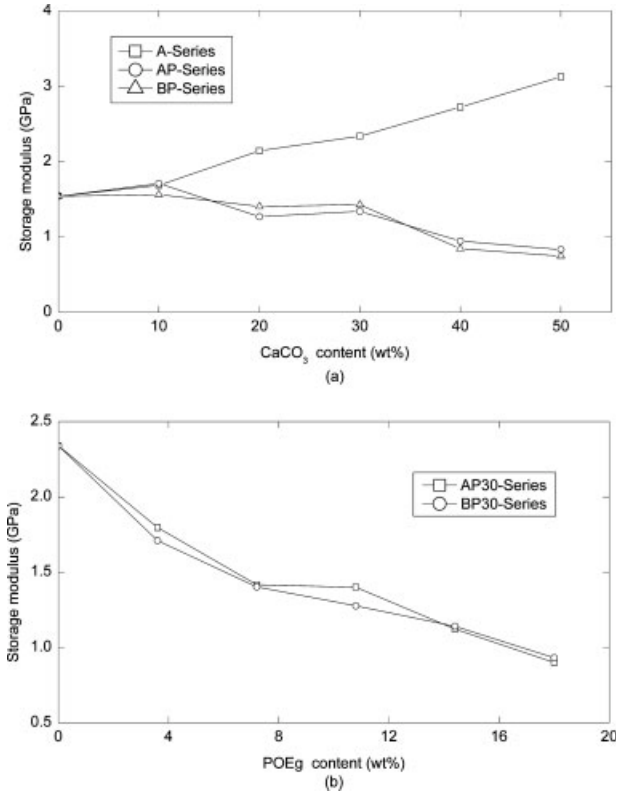

Figure 7 Influence of the $CaCO_3$ and POEg content on the storage modulus at room temperature.

The DSC data for neat HDPE and the A, AP, and BP series and the influence of the $CaCO_3$ content on the crystallization behavior are presented in Figure 8. The incorporation of $CaCO_3$ particles into HDPE (A series) has some influence on the nucleation of polyethylene crystallites by increasing the crystallization temperature (T_c). This indicates that $CaCO_3$ particles act as nucleating agents, promoting the crystallization of HDPE at the surface and hence leading to a slightly higher T_c. Also,

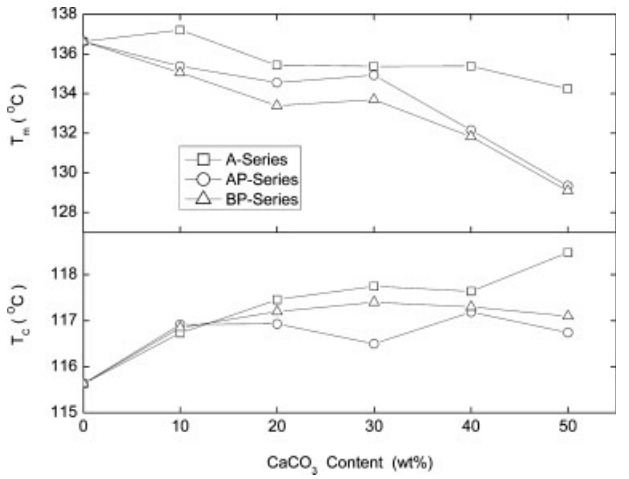

Figure 8 Influence of the $CaCO_3$ content on T_m and T_c of the A, AP, and BP series.

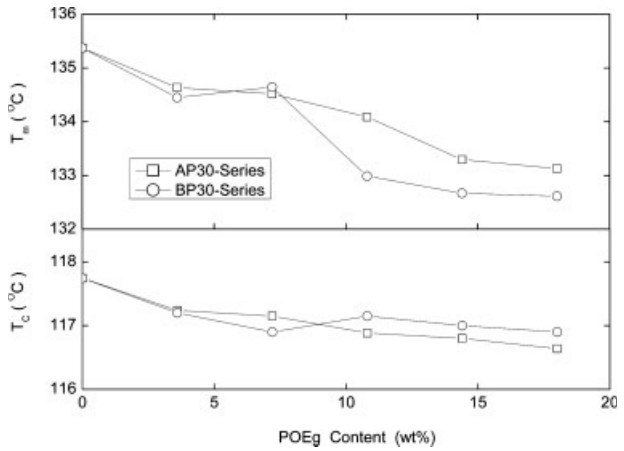

Figure 9 Influence of the POEg content on T_m and T_c of the AP30 and BP30 series.

for all blends of the A series, the melting temperature (T_m) decreases slightly as the $CaCO_3$ content increases. On the basis of the classical thermodynamic model for crystallite free energy, this decrease in T_m indicates that the HDPE lamellae in the vicinity of the $CaCO_3$ particles are thinner than those in neat HDPE. These results confirm those in a previous work by Bartczak et al.,[2] who used an HDPE grade with similarly coarse $CaCO_3$ particles.

The influence of the rubber phase and particle treatment on the melting point and crystallization of the blends is also systematically examined in Figure 8. The DSC data for the AP and BP series in Figure 8 show that T_m is lower than that of A series and decreases gradually before the $CaCO_3$ content increases to 30% and remarkably after that. The rapid decrease in T_m of the last two samples in the AP and BP series may be related to the much thinner HDPE lamellae in these blends. In these blends, the HDPE content is much lower (42 and 27.5%, respectively). $CaCO_3$ and POEg inhabit most of the blends and penetrate the HDPE matrix, and this means that the crystal is not perfect and that the thickness of the HDPE lamellae is much thinner. Thus, it melts at a lower temperature. On the other hand, T_c is also slightly lower than that of the A series. It has been found that in HDPE/POE binary blends, the incorporation of POE into HDPE has little influence on T_m or T_c.[15] Because the AP and BP series blends are characterized by a fixed POEg/$CaCO_3$ weight ratio, it seems that the role of POEg is more important than that of $CaCO_3$ particles as the filler content increases. The DSC results for the ternary blends in Figure 8 should be related not only to the components but also to the composite morphology. The DSC technique has been successfully used to characterize the morphology of PP/POEg/$CaCO_3$ ternary blends by the analysis of the influence of the composition on T_c and T_m.[8,12] However, because of the separate weak influence of the $CaCO_3$ particle and rubber phase on the crystallization behavior of HDPE, in light of the synergistic effects of the fillers on T_c in Figure 8, it is not capable of revealing the morphology in the HDPE/POEg/$CaCO_3$ blends (with a fixed POEg/$CaCO_3$ ratio), which is revealed in the section on SEM analysis.

The detailed influence of POEg on the crystallization behavior of blends with a fixed concentration of $CaCO_3$ particles (30 wt %) is displayed in Figure 9, which was obtained with samples of the AP30 and BP30 series. Both T_m and T_c decrease before the POEg content increases to 10.8% and somehow reach stability after that; this indicates that POEg plays an important role in the crystallization behavior. In comparison with a binary blend, a separate dispersion of $CaCO_3$ particles and POEg in the polymers has no influence on the crystallization behavior of the matrix.[12] Therefore, it seems that the result shown in Figure 9 indicates that a core–shell structure is formed in the ternary blends. Although T_c of the HDPE matrix is raised by mineral particles, the introduction of a POEg interphase that covers the surface of the $CaCO_3$ particles presumably shields the nucleating effect of the mineral phase, so that the overall crystallization is hindered. When the POEg content is high enough, all the particles are covered, and the crystallization is stabilized.

The results obtained from the materials reinforced with treated $CaCO_3$ particles versus those with untreated particles are also compared (Figs. 8 and 9). The discrepancy between the blends containing treated $CaCO_3$ particles and those containing untreated particles is very small, mostly less than 0.5°C. As detailed in Figure 1, the treatment layer at the surface of $CaCO_3$ reacts with POEg. Its main influence is to improve the adhesion between the $CaCO_3$ filler and rubber phase. Thus, it is considered that the treatment of the $CaCO_3$ particle has a negligible influence on the kinetics of crystallization of polyethylene.

SEM analysis

SEM micrographs of the cryofractured surfaces of binary and ternary blends (nonetched and etched) containing 10 wt % $CaCO_3$ particles are shown in Figure 10. The nonetched fractured surface of blend AP10 has a better interface near the $CaCO_3$ particle than that of A10 [Fig. 10(a,b)]. Compared with Figure 10(b), the surface etched by normal heptane [Fig. 10(c)] shows a thin void layer at the surface of the $CaCO_3$ particles, which confirms that a core–shell structure is formed in the ternary blends. Also, at a higher magnification, Figure 11(b) shows in the BP30-1 blend a narrow void layer at the surface of the particle in the etched specimen. This void layer is definitely absent in the micrograph obtained without etching [Fig. 11(a)]. This observation proves again that a POEg shell is formed at the interface between the $CaCO_3$ particles and the HDPE matrix in the ternary blends.

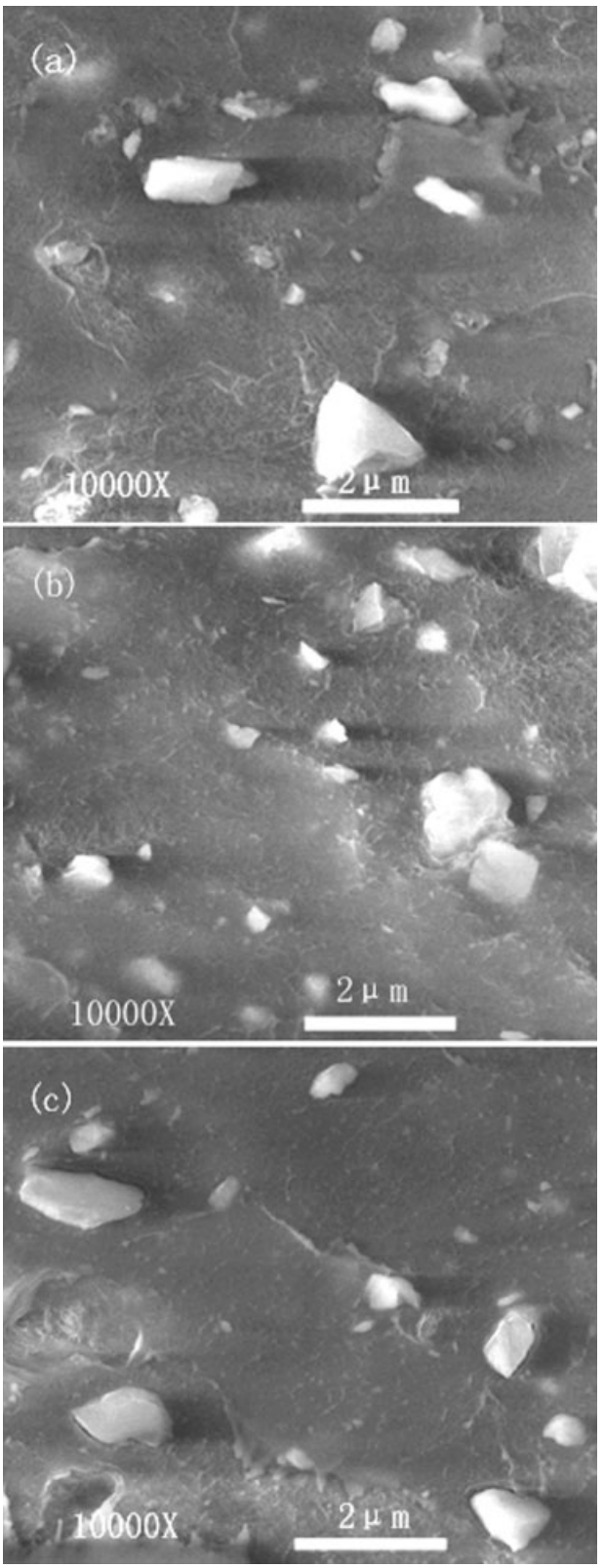

Figure 10 Cryofractured surfaces of blends containing 10 wt % $CaCO_3$ particles: (a) A10, (b) AP10 (nonetched), and (c) AP10 (etched).

The micrographs in Figure 12 present the microstructures of etched cryofractured surfaces from the A40 and AP40 blends, in which the mineral fraction is high (40 wt % $CaCO_3$). In the binary blend [Fig. 12(a)], the particles show significant interfacial debonding; no void layer appears in the ternary blend [Fig. 12(b)] even though it was etched. Because cryofractured surfaces are exposed via a brittle fracture process, this unexpected feature should be ascribed to the specific rupture behavior of the AP40 blend. In the work of Xie et al.,[19] also devoted to HDPE/POEg/$CaCO_3$ blends with a fixed POEg/$CaCO_3$ ratio, the authors found a brittle–tough transition when the $CaCO_3$ content became larger than 20 wt %. Actually, in this series, the significant parameter is not the $CaCO_3$ concentration itself but rather is the related POEg fraction. As such, in light of the criterion introduced by Wu,[20] blends with high volume fractions of a core–shell structure exhibit high toughness, and the fracture propagates entirely within the

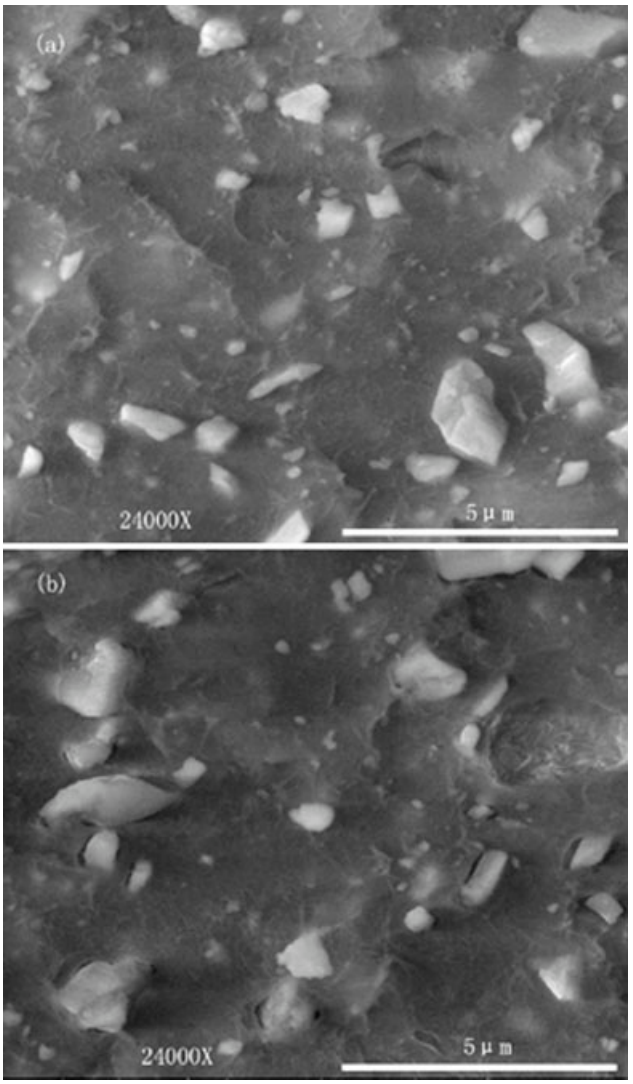

Figure 11 Cryofractured surfaces of the BP30-1 blend: (a) nonetched and (b) etched.

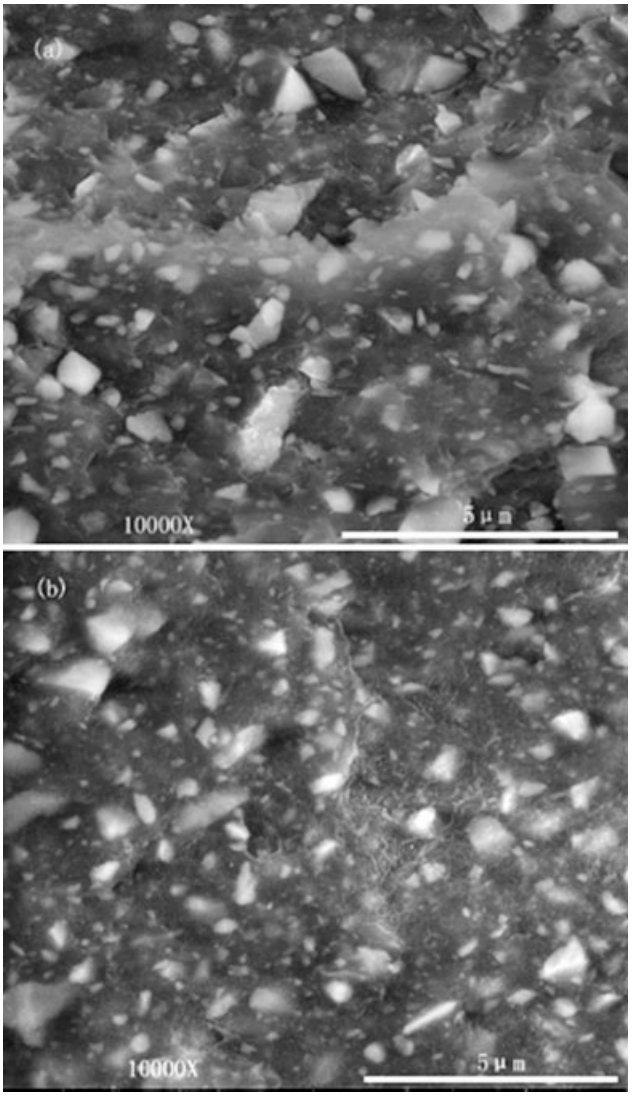

Figure 12 Cryofractured surfaces of blends containing 40 wt % $CaCO_3$ particles: (a) A40 and (b) AP40 (etched).

matrix, without exposing rubber particles. Consequently, in the micrograph of Figure 12(b), the cryofractured surface of the AP40 blend lies in the HDPE matrix, which protected the POEg interphase from the attack of the etching agent.

As stated, this effect of the particle treatment on the morphology is not noticeable in the SEM observations, which reveal almost no effect of the $CaCO_3$ treatment on the morphology of the ternary blends. Actually, the main influence of the $CaCO_3$ treatment is to improve the adhesion between the $CaCO_3$ filler and POEg and consequently to increase the yield stress and the impact strength.[18,19] Besides that, the filler treatment has very little influence on the morphology of the blends.

CONCLUSIONS

In this work, the dynamic mechanical properties, the crystallization behavior, and the morphology of five series of HDPE/$CaCO_3$ blends with and without POEg have been investigated. The storage modulus of the blends significantly increases with increasing $CaCO_3$ content, whereas the influence of POEg on the modulus is mainly determined by T_g of POEg. The crystallization behavior of the ternary blends depends on not only the composition but also the morphology, which is a core–shell structure in the ternary blends. The treatment of $CaCO_3$ particles with an amino acid has limited influence on the viscoelastic behavior of the blends or the morphology.

References

1. Gao, Z. J.; Tsou, A. H. J Polym Sci Part B: Polym Phys 1999, 37, 155.
2. Bartczak, Z.; Argon, A. S.; Cohen, R. E.; Weinberg, M. Polymer 1999, 40, 2347.
3. Liu, Z. H.; Kwok, K. W.; Li, R. K. Y.; Choy, C. L. Polymer 2002, 43, 2501.
4. Thio, Y. S.; Argon, A. S.; Cohen, R. E.; Weinberg, M. Polymer 2002, 43, 3661.
5. Wang, Y.; Wang, J. J Polym Eng Sci 1999, 39, 190.
6. Wilbrink, M. W. L.; Argon, A. S.; Cohen, R. E.; Weinberg, M. Polymer 2001, 42, 10155.
7. Suwanprateeb, J.; Tiemprateeb, S.; Kangwantrakool, S.; Hemachandra, K. J Appl Polym Sci 1998, 70, 1717.
8. Premphet, K.; Horanont, P. Polymer 2000, 41, 9283.
9. Hornsby, P. R.; Premphet, K. J Appl Polym Sci 1998, 70, 587.
10. Yu, Z. Z.; Lei, M.; Ou, Y. C.; Yang, G. S.; Hu, G. H. J Polym Sci Part B: Polym Phys 2000, 38, 2801.
11. Wang, Y.; Lu, J.; Wang, G. H. J Appl Polym Sci 1997, 64, 1275.
12. Premphet-Sirisinha, K.; Preechachon, I. J Appl Polym Sci 2003, 89, 3557.
13. Bensason, S.; Nazarenko, S.; Chum, S.; Hiltner, A.; Baer, E. Polymer 1997, 38, 3513.
14. Bensason, S.; Nazarenko, S.; Chum, S.; Hiltner, A.; Baer, E. Polymer 1997, 38, 3913.
15. Bartczak, Z.; Argon, A. S.; Cohen, R. E.; Weinberg, M. Polymer 1999, 40, 2331.
16. Bai, S. L.; G'Sell, C.; Hiver, J. M.; Mathieu, C. Polymer 2005, 46, 6437.
17. Yang, J. H.; Zhang, Y.; Zhang, Y. X. Polymer 2003, 44, 5047.
18. Yang, Y. L.; G'Sell, C.; Hiver, J. M.; Bai, S. L. Polym Eng Sci, in press.
19. Xie, T. X.; Liu, H. Z.; Ou, Y. C.; Yang, G. S. J Polym Sci Part B: Polym Phys 2005, 43, 3213.
20. Wu, S. J Appl Polym Sci 1988, 35, 549.